

Charge dynamics of a double-exchange ferromagnet $\text{La}_{1-x}\text{Sr}_x\text{MnO}_3$

K. Takenaka,* R. Shiozaki, and S. Sugai

Department of Physics, Nagoya University, Nagoya 464-8602, Japan

(Received 15 December 2001; published 13 May 2002)

We have investigated the charge dynamics of the doped carriers in a prototypical double-exchange ferromagnet $\text{La}_{1-x}\text{Sr}_x\text{MnO}_3$ by reflectivity measurements on cleaved surfaces of the single crystals. Even for wide-band $\text{La}_{0.6}\text{Sr}_{0.4}\text{MnO}_3$, which shows a metallic dc resistivity over the entire temperature range up to 1000 K, the optical conductivity $\sigma(\omega)$ deviates from a simple Drude response; it shows a slowly decaying ($\propto \omega^{-1}$) quasi-Drude behavior below a certain temperature T^* , while above T^* it is characterized by a finite-energy peak instead of the Drude peak. Al substitution affects $\sigma(\omega)$ over a wide energy range up to 1 eV or higher, which is contrary to the prediction from the simple Drude picture. These characteristics can be well described by the one-component description.

DOI: 10.1103/PhysRevB.65.184436

PACS number(s): 75.30.Vn, 78.20.-e, 71.27.+a

I. INTRODUCTION

It is commonly observed for a variety of transition-metal compounds that the optical conductivity $\sigma(\omega)$ in the metallic phase does not obey a simple Drude description $\sigma(\omega) = \omega_p^2 \gamma / 4\pi(\omega^2 + \gamma^2)$ (ω_p : plasma frequency; γ : scattering rate),¹ but shows a slowly decaying “quasi-Drude” behavior.²⁻⁴ This has been considered as a clue for understanding the electronic states and the dynamics of the charge carriers doped onto a Mott insulator, which are central concerns in the recent condensed-matter physics, and in the last decade a lot of experimental as well as theoretical effort has been put into elucidating the origin of the quasi-Drude response. On this issue, typically for the normal state of high-temperature superconducting cuprates, there has a long-standing dispute on whether this quasi-Drude response is interpreted as a single collective mode described by an extended Drude formula with a frequency-dependent scattering rate γ^* and optical mass m^* (*one-component picture*) or as a superimposition of a simple Drude peak and a broad infrared (IR) band (*two-component picture*).⁵

Also for manganese perovskites, which have attracted renewed interest because of their intriguing phenomena of colossal magnetoresistance (CMR),⁶ $\sigma(\omega)$ in the ferromagnetic-metallic state is characterized by a similar quasi-Drude peak.⁷⁻¹⁷ The optical spectra of the manganites have been frequently used as the experimental basis of the theories¹⁸⁻³¹ that are proposed in order to explain the various peculiar phenomena of these compounds including CMR, but the earlier reflectivity measurements were analyzed mostly using the two-component picture. Because those results were obtained on the surfaces damaged by polishing, they may provide a distorted view of the intrinsic properties. In the present paper, the $\sigma(\omega)$ spectra of the ferromagnetic-metallic manganites obtained on *cleaved* surfaces of the single crystals are examined using the one-component picture. The one-component description has played an important role in understanding the physical properties of high-temperature superconductors. In particular, it provides a better description of the pseudogap behavior in the underdoped cuprates.³²⁻³⁵

First, we show the result of the reflectivity study on the

wide-band $\text{La}_{0.6}\text{Sr}_{0.4}\text{MnO}_3$, which shows a metallic dc resistivity $\rho(T)$ over the entire temperature T range up to 1000 K. Even for this highly doped compound that has been considered to obey the simple double-exchange mechanism,¹⁸ $\sigma(\omega)$ deviates from its prediction; $\sigma(\omega)$ is characterized by a finite-energy peak, instead of a Drude peak at $\omega=0$, above a certain temperature T^* , which is lower than the Curie temperature T_C . Below T^* , $\sigma(\omega)$ shows the slowly decaying quasi-Drude behavior similar to other correlated metals, and this feature can be well described by the monotonic ω -linear γ^* over a wide energy range up to several 1000 cm^{-1} . Second, we show the impurity effect on $\sigma(\omega)$. The Al doping affects $\sigma(\omega)$ over the entire energy range up to 1 eV or higher, which is at odds with the prediction of the simple Drude picture. In the slightly Al-doped region, where $\rho(T)$ remains metallic, the characteristic ω linearity of γ^* at low temperatures is not altered. The above results suggest that the two-component picture is artificial as the interpretation of the quasi-Drude behavior, because the two-component picture assumes that the charge dynamics obeys the simple Drude response. Instead, the quasi-Drude behavior can be naturally interpreted from the one-component picture. We discuss the relation between the crossover in $\sigma(\omega)$ and the “bad metallic” resistivity,³⁶⁻³⁸ or the absence of the resistivity saturation even at the Mott criterion σ_{Mott} , in which the mean free path l is comparable with the Fermi wavelength $\lambda_F = 2\pi/k_F$.³⁹ The present experiment suggests that the crossover in $\sigma(\omega)$ is relevant to the Mott criterion in dc conductivity. The finite-energy peak is a possible indication of the “dynamical” localization.

II. EXPERIMENTS

All of the samples used here were the single crystals grown by a floating-zone method.⁴⁰ The obtained crystals are cylindrical in shape, typically 6 mm in diameter and 8 cm in length. Inductively couple plasma spectroscopy of the obtained crystals confirmed the chemical composition to be identical to the starting compositional ratio. The measurements of $\rho(T)$ were performed using a conventional four-probe method. The crystal was cut into a rectangular shape (typically $4 \times 1 \times 0.5 \text{ mm}^3$). For $\text{La}_{0.6}\text{Sr}_{0.4}\text{MnO}_3$, after the

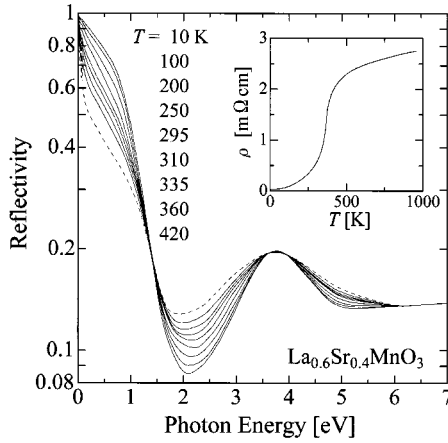


FIG. 1. Temperature-dependent optical reflectivity spectra $R(\omega)$ measured on cleaved surfaces of $\text{La}_{0.6}\text{Sr}_{0.4}\text{MnO}_3$ ($T_C=366$ K). Dashed line represents the data taken at 420 K. Inset shows the dc resistivity $\rho(T)$ up to 1000 K.

electrodes were formed with heat-treatment-type gold paste, $\rho(T)$ was measured in the range 4.2–1000 K. The high-temperature measurements above 300 K were conducted under flowing oxygen gas to avoid increasing oxygen deficiencies. Our previous study ensured that physical properties are not affected for $x \geq 0.3$ by the above procedure of $\rho(T)$ measurement.⁴¹ Actually, there was no difference between the $\rho(T)$ values at 300 K measured before and after heating up to 1000 K. For $(\text{La}_{0.825}\text{Sr}_{0.175})(\text{Mn}_{1-z}\text{Al}_z)\text{O}_3$, the electrodes were formed by ultrasonic soldering of indium and $\rho(T)$ was measured below 400 K. For each composition, we measured $\rho(T)$ of several samples in order to verify that the scattering of the data was within the dimensional error ($\pm 4\%$). The Curie temperature T_C determined by $\rho(T)$ is 366 K ($x=0.4$), 283 K ($x=0.175$, $z=0$), and 273 K ($x=0.175$, $z=0.01$). The details of the resistivity measurement are described elsewhere.^{37,41,42}

Near-normal incident reflectivity $R(\omega)$ spectra were measured on the cleaved surfaces with a flat area of typically 1×1 mm² using a Fourier-type interferometer Bomem DA8 (0.005–1.6 eV), a grating spectrometer Jobin Yvon TRIAX180 (0.8–6.6 eV), and a Seya-Namioka type spectrometer for vacuum-ultraviolet synchrotron radiation (4.0–40 eV) at the Institute for Molecular Science, Okazaki National Research Institutes. As a reference mirror, we used an evaporated Au (far- to near-IR regions) and Ag (visible region) film on a glass plate. The experimental error of the reflectivity ΔR , determined from the reproducibility, is less than 1% for the far-IR to visible regions and less than 2% for the ultraviolet to vacuum-ultraviolet regions.

III. RESULTS

A. Overall features

The temperature-dependent (10–420 K) reflectivity spectra measured on cleaved surfaces of $\text{La}_{0.6}\text{Sr}_{0.4}\text{MnO}_3$ single crystal are shown in Fig. 1 on a logarithmic R scale. The dashed line represents the data at 420 K. As temperature

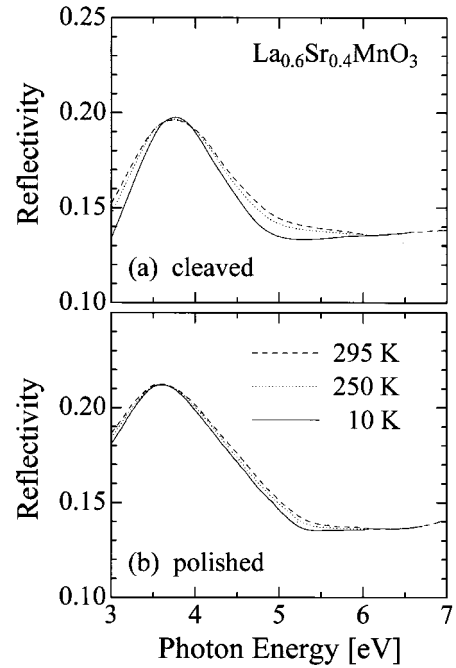


FIG. 2. Temperature dependence of reflectivity at 3–7 eV measured on cleaved (a) and polished (b) surfaces of $\text{La}_{0.6}\text{Sr}_{0.4}\text{MnO}_3$; solid line, 10 K, dotted line, 250 K; dashed line, 295 K.

decreases, the reflectivity edge at ≈ 1.6 eV becomes sharper and the optical phonons are screened, which are consistent with the metallic resistivity ($d\rho/dT > 0$) (inset of Fig. 1). For this highly doped (or wide-band) manganite, $\rho(T)$ is metallic over the entire temperature range covered here. In addition, one should note that the present spectra exhibit temperature dependence up to ~ 6 eV, which is much larger than that of the other strongly correlated materials, which is at most ~ 3 eV.⁴

Because the $R(\omega)$ spectra of the ferromagnetic-metallic manganese perovskites are quite sensitive to the surface deterioration, cleaved surfaces are indispensable for obtaining reliable spectra.⁴³ We have reported that for the room-temperature data, the reflectivity around the edge is highly suppressed by deterioration of the sample surfaces and the spectrum taken at the cleaved surface shows the much sharper edge and the much higher reflectivity in this energy region, which produces the pronounced quasi-Drude peak with a much larger spectral weight in $\sigma(\omega)$.⁴⁴ Here we show the effect of the surface deterioration on the temperature dependence of $R(\omega)$ at higher-energy regions. The spectrum measured on the cleaved surfaces [Fig. 2(a)] exhibits temperature dependence up to 6 eV much more clearly than the spectrum measured on polished surfaces [Fig. 2(b)]. The deterioration of the sample surfaces may have concealed the temperature dependence above 4 eV in the previous studies. Actually, the optical absorption study,⁸ which is less sensitive to the surface, suggests that the temperature dependence of $\sigma(\omega)$ extends up to the upper limit of their measurements (5 eV). In addition, their experiment indicates that the integrated spectral weight of $\sigma(\omega)$ does not converge even at 5 eV.

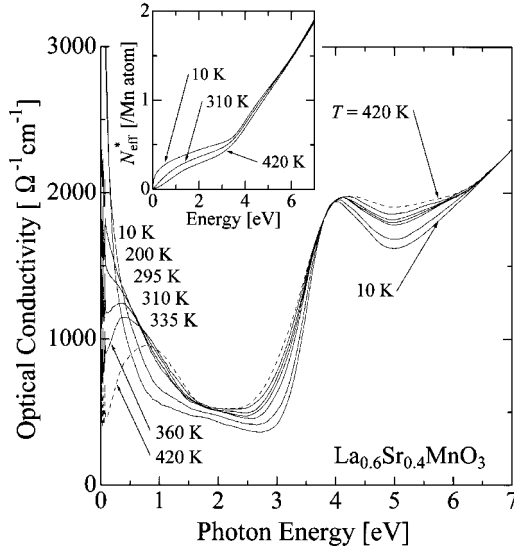


FIG. 3. Temperature-dependent optical conductivity spectra $\sigma(\omega)$ of $\text{La}_{0.6}\text{Sr}_{0.4}\text{MnO}_3$ deduced from $R(\omega)$ (shown in Fig. 1) via a Kramers-Kronig transformation. Dashed line represents the spectrum at 420 K. The data at 100 K and 250 K are not shown for clarity. Inset shows the effective carrier number $N_{\text{eff}}^*(\omega)$ defined as the integration of $\sigma(\omega)$.

In order to facilitate a more detailed and quantitative discussion, we deduce optical conductivity $\sigma(\omega)$ (Fig. 3) from $R(\omega)$ shown in Fig. 1 via a Kramers-Kronig (KK) transformation. We measured the $R(\omega)$ spectra at each temperature below 6.6 eV, and above 6.6 eV we assumed the data measured at room temperature (295 K). Such a procedure is possible and reasonable because the temperature variation of $R(\omega)$ in the range 6.0–6.6 eV was negligibly small and the connection was smooth. In addition, the integrated spectral weight defined as

$$N_{\text{eff}}^*(\omega) = \frac{2m_0V}{\pi e^2} \int_0^\omega \sigma(\omega') d\omega' \quad (1)$$

(m_0 : bare-electron mass; V : unit-cell volume) almost converges ($\Delta N_{\text{eff}}^*/N_{\text{eff}}^* \lesssim 2\%$) at 6.6 eV (inset of Fig. 3). This also seems to support our analytical procedure.

For the extrapolation at the low-energy part, we assumed a Hagen-Rubens reflectivity. The extrapolating parameter $\sigma(0)$ is coincident with the measured dc value $\sigma_{\text{dc}} = \rho^{-1}$ within the dimensional error of the resistivity measurement. Although variation of the extrapolation procedures has a small effect on the absolute value of $\sigma(\omega)$ in the energy region 10–20 meV, the qualitative behavior (or ω dependence) of $\sigma(\omega)$ summarized below is not affected. Above 20 meV the spectrum is not affected by variation of the extrapolation procedures.

The temperature-dependent part of the $\sigma(\omega)$ spectrum can be separated into three regions, the (0–2)-eV, (2–4)-eV, and (4–7)-eV regions. This T -dependent part is piled on the T -independent background consisting of interband transitions such as the charge-transfer excitations from O $2p$ to Mn $3d$ or La/Sr $5d$.¹⁶ The spectral weight at the

(2–4)- and (4–7)-eV regions decreases with decreasing temperature. The missing spectral weight is transferred to the lowest-energy region and forms a collective excitation of the charge carriers. Because the spectral weight in the (2–4)-eV region compensates for *only half* of the spectral weight associated with the lowest-energy intraband excitation, our result showing the temperature dependence up to 6 eV is reasonable also in terms of the f -sum rule. This transfer of spectral weight is predicted from the dynamical mean-field theory of the double-exchange model.¹⁸ In this scenario, the spectral weight at the two higher-lying regions is ascribed to what is called “exchange-gap” excitations; the (2–4)-eV region, $e_g \uparrow \rightarrow t_{2g} \downarrow$; the (4–7)-eV region, $e_g \uparrow \rightarrow e_g \downarrow$ and $t_{2g} \uparrow \rightarrow t_{2g} \downarrow$.^{16,45} In this paper, we focus the argument on the lowest-energy collective mode or the dynamics of the charge carriers. The higher-energy parts of $\sigma(\omega)$ have been already discussed in the previous works.^{16,42}

One of the most significant features is that $\sigma(\omega)$ exhibits a finite-energy peak, instead of a Drude peak, above a certain temperature T^* , which is about room temperature, though $\rho(T)$ remains metallic even above T^* . In the simple Drude formalism, no matter how strong the scattering becomes, $\sigma(\omega)$ only approaches asymptotically ω -independent (flat) conductivity and peaks still at $\omega=0$. The present *coherent-to-incoherent crossover* suggests the breakdown of the simple Drude picture as well as some critical change in the charge transport around T^* . It is noteworthy that T^* is lower than T_C . The characteristic change in $\sigma(\omega)$ occurs not at T_C but at T^* , though $\rho(T)$ exhibits the anomaly at T_C .

Another characteristic feature is the Drude peak below T^* . This peak decays more slowly ($\propto \omega^{-1}$) than the simple Drude response ($\propto \omega^{-2}$) and consequently the width is much larger (~ 1 eV) than that of ordinary metals (at most, several times of $k_B T$).⁴⁶ The width decreases somewhat with decreasing temperature, but the simple Drude response is not recovered even at the lowest temperature. This quasi-Drude peak is commonly observed for almost all correlated metals. This is the origin of the long-standing dispute, whether the one-component or the two-component picture is more reasonable. For the manganites, the two-component picture has been regarded so far as if it were the experimental result. However, those arguments were based on the wrong reflectivity spectra obtained on the damaged surface. Such damages cannot be completely removed even by annealing after polishing.^{12,43} Also for the manganites, the two-component picture is *not the experimental result but one of the possible interpretations*. The pronounced quasi-Drude peak observed in the present reflectivity study using cleaved surfaces is consistent with the optical absorption studies.^{7,8,13} In addition, Quijada *et al.* also suggested a similar coherent-to-incoherent crossover in $\sigma(\omega)$ in Ref. 8. Here, we show that the optical spectra of the manganites can be more reasonably interpreted from the one-component picture.

B. One-component approach

The present analysis follows the extended Drude formalism by Webb, Sievers, and Mihalisin,⁴⁷

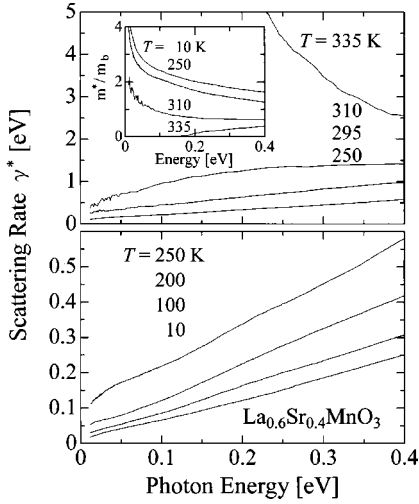


FIG. 4. Frequency-dependent (renormalized) scattering rate γ^* of $\text{La}_{0.6}\text{Sr}_{0.4}\text{MnO}_3$ calculated via an extended Drude analysis; top panel, $T=250\text{--}335$ K, bottom panel, $T=10\text{--}250$ K. Inset shows the frequency-dependent effective-mass ratio m^*/m_b .

$$\hat{\sigma}(\omega) = \left(\frac{\omega_p^2}{4\pi} \right) \frac{1}{\hat{\gamma}(\omega) - i\omega}, \quad (2)$$

$$\omega_p^{*2} = \frac{\omega_p^2}{1 + \lambda(\omega)}, \quad (3a)$$

$$\gamma^* = \frac{\text{Re } \hat{\gamma}}{1 + \lambda(\omega)} = \left(\frac{\omega_p^2}{4\pi} \right) \text{Re} \left(\frac{1}{\hat{\sigma}} \right) \frac{1}{1 + \lambda(\omega)}, \quad (3b)$$

$$\frac{m^*}{m_b} = 1 + \lambda(\omega) = 1 - \frac{1}{\omega} \text{Im } \hat{\gamma} = - \left(\frac{\omega_p^2}{4\pi} \right) \text{Im} \left(\frac{1}{\hat{\sigma}} \right) \frac{1}{\omega}. \quad (3c)$$

Plasma frequency ω_p is defined as $\omega_p^2 = 4\pi n e^2 / m_b$ (n : carrier density; m_b : high-frequency optical mass). $\hat{\sigma}(\omega)$ is complex conductivity and relates to the complex dielectric function $\hat{\epsilon}(\omega)$ as $\hat{\epsilon}(\omega) = \epsilon_\infty + (4\pi/\omega)\hat{\sigma}(\omega)i$. $\sigma(\omega)$ is defined as $\sigma(\omega) = \text{Re } \hat{\sigma}(\omega) = (\omega/4\pi)\text{Im } \hat{\epsilon}(\omega)$. ω_p^* , γ^* , and m^*/m_b are the *renormalized* plasma frequency, *renormalized* scattering rate, and mass-enhancement ratio, respectively. In this formalism, the Drude formula is generalized as $\sigma(\omega) = \omega_p^{*2} \gamma^* / 4\pi(\omega^2 + \gamma^{*2})$. In the simple Drude formula, γ^* is independent of ω (but depends on T) and m^*/m_b is equal to unity. The real and imaginary parts of the complex scattering rate $\hat{\gamma}$, that is, $\text{Re } \hat{\gamma} = \gamma(\omega)$ (*unrenormalized* scattering rate) and $-\text{Im } \hat{\gamma}/\omega = \lambda(\omega)$, are constrained by a KK relation. In the limit of zero frequency, $\gamma^*(\omega)$ approaches the dc scattering rate and $\text{Im } \hat{\gamma}(\omega)$ tends to zero. The parameter ω_p is estimated by the f -sum rule $\int_0^\infty \sigma(\omega) d\omega = (1/8)\omega_p^2$.

Figure 4 shows $\gamma^*(\omega)$ (main panels) and $m^*(\omega)/m_b$ (inset) of $\text{La}_{0.6}\text{Sr}_{0.4}\text{MnO}_3$ below 0.4 eV. The contribution from the optical phonons is subtracted and hence the spectra below 0.02 eV are noisy and contain some ambiguity. The contribution from the interband excitations is negligible below 0.4 eV.^{7,16} Therefore, the spectra shown in Fig. 4 are the

contributions almost purely from the charge carriers. ω_p is determined by the area contained in $\sigma(\omega)$ up to the reflectivity edge 1.6 eV. This value increases with decreasing temperature (inset of Fig. 3), especially in the vicinity of T_C , corresponding to the spectral-weight transfer from the exchange-gap excitations to the intraband excitation. [ω_p is $25\,000\text{ cm}^{-1}$ (10 K) and $22\,500\text{ cm}^{-1}$ (310 K).] The decrease in ω_p suppresses m^*/m_b in the relation $m^*/m_b \propto \omega_p^2$. Such a drastic change in ω_p with T is a unique character of the manganites. Because the ω_p value is defined as the spectral weight up to 1.6 eV in the present case and hence contains the contribution from the interband excitations, the absolute values of m^*/m_b are somewhat arbitrary. (Note that γ^* is independent of ω_p .) ϵ_∞ is chosen to be 3. Variation of ϵ_∞ does not affect γ^* or m^*/m_b below 0.4 eV.

The extended Drude analysis more clearly exposes the variation of the charge dynamics with temperature. In the low- T coherent region, γ^* exhibits the characteristic ω -linear behavior over a wide energy range up to 0.4 eV. m^*/m_b shows enhancement at low frequencies, but decreases as ω increases and approaches unity asymptotically at high frequencies. These characteristics are not essentially altered with T in the coherent region; with increasing temperature, γ^* keeps its ω linearity, though both the slope and section of it increase, and m^*/m_b only slightly decreases. These features are similar to those of an optimally doped cuprate superconductor in the normal state.^{4,5,35} However, at 310 K γ^* deviates from the ω -linear behavior and m^*/m_b is so suppressed that it does not reach unity even at 0.4 eV, though the signs of $d\gamma^*/d\omega$ and $dm^*/d\omega$ are identical to those at lower temperatures. The crossover begins even at 310 K, where $\sigma(\omega)$ barely shows a zero-energy peak. In the high- T incoherent region (at 335 K in Fig. 4), γ^* increases divergently with decreasing ω and m^*/m_b falls and passes zero in the same ω region. These nonmonotonic behaviors are unusual and seem to be beyond even the ω -dependent scattering description of the coherent motion.

C. Impurity effect

We have investigated the Al-doping effect on the optical spectra. The Al atom substituted for the Mn atom is expected to act simply as a defect in the double-exchange system because it is trivalent and in the closed-shell configuration.^{37,42} In the simple Drude picture, a defect (or an impurity atom) acts as an elastic scatterer and increases $\gamma = \hbar/\tau$, which widens the Drude peak (but does not affect the spectral weight).¹ Therefore, if the two-component picture is reasonable, the effect of Al doping is expected to be limited below a low-energy region ($\sim k_B T$), because the two-component picture assumes that the charge dynamics obeys the simple Drude response.

Figure 5 shows $\sigma(\omega)$ for $(\text{La}_{0.825}\text{Sr}_{0.175})(\text{Mn}_{1-z}\text{Al}_z)\text{O}_3$ ($z=0$ and 0.01). These spectra were obtained via a KK transformation from $R(\omega)$ measured on the cleaved surfaces. The $R(\omega)$ spectra are not shown because that of the Al-free crystal has been already reported^{12,16} and the overall feature is almost the same as that of $\text{La}_{0.6}\text{Sr}_{0.4}\text{MnO}_3$ shown in Fig. 1. The inset of Fig. 5 shows $\rho(T)$ for these two compounds.

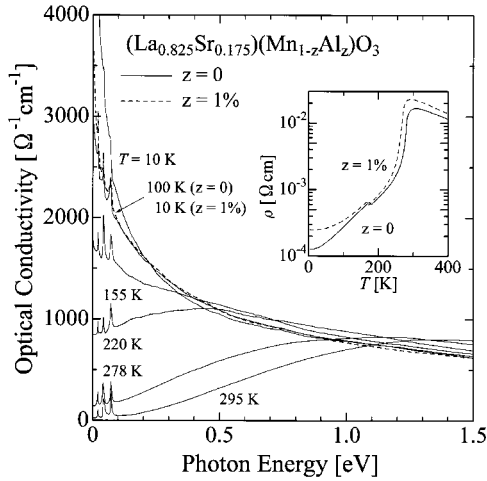


FIG. 5. Temperature-dependent optical conductivity spectra $\sigma(\omega)$ of $(\text{La}_{0.825}\text{Sr}_{0.175})(\text{Mn}_{1-z}\text{Al}_z)\text{O}_3$ for $z=0$ (solid line) and $z=1\%$ (dashed line). Inset shows the dc resistivity $\rho(T)$ up to 400 K.

Solid and dashed lines represent the $z=0$ and $z=0.01$ data, respectively. Similar to the $x=0.4$ compound, the $\sigma(\omega)$ spectra of the Al-free compound show the coherent-to-incoherent crossover. T^* is about 200 K in this case, which is lower than $T_C=283$ K. For $x=0.175$, $\rho(T)$ exhibits the insulating behavior ($d\rho/dT < 0$) above T_C , but the essential feature of the optical spectra is independent of whether $\rho(T)$ is metallic or insulating above T_C . $\sigma(\omega)$ of 1% Al-doped compound at 10 K is almost coincident with that of the Al-free compound at 100 K over a wide energy range up to 1 eV or higher, which covers the entire range relevant to the charge dynamics. In addition, γ^* of the Al-free $x=0.175$ compound (Fig. 6) shows the ω -linear behavior similar to the $x=0.4$ compound at low temperatures. γ^* of the 1% Al-doped compound at 10 K (dashed line) also coincides with γ^* of the Al-free compound at 100 K. The resistivity measurement shows that σ_{dc} of the 1% Al-doped compound at 10 K is almost identical to that of the Al-free compound at 100 K. For the double-exchange manganites, the overall feature of the charge dynamics up to 1 eV or higher seems to be dominated by σ_{dc} , unless the doped Al destroys the metallic state.⁴² The above features are incompatible with the simple Drude response.

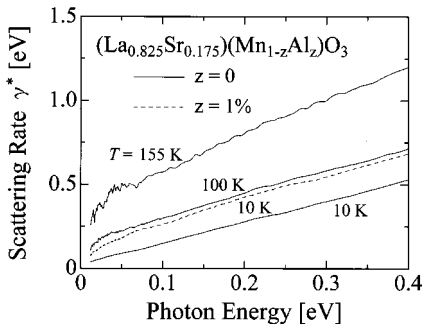


FIG. 6. Frequency-dependent (renormalized) scattering rate γ^* of $(\text{La}_{0.825}\text{Sr}_{0.175})(\text{Mn}_{1-z}\text{Al}_z)\text{O}_3$ calculated via an extended Drude analysis for $z=0$ (solid line) and $z=1\%$ (dashed line).

IV. DISCUSSION

A. One-component vs two-component response

The present experimental results indicate that the one-component picture more reasonably describes the charge dynamics in the ferromagnetic-metallic state of the doped manganites. The reason why is summarized as follows.

(1) The finite-energy peak in $\sigma(\omega)$ can hardly be explained by the simple Drude model. Because the finite-energy peak continuously and smoothly changes to the quasi-Drude peak, it seems to be artificial that the charge dynamics immediately recovers the simple Drude response when the peak shifts to zero frequency.

(2) The present coherent-to-incoherent crossover can be described systematically by the frequency-dependent scattering rate $\gamma^*(\omega)$ deduced from the extended Drude analysis. In particular, $\gamma^*(\omega)$ exhibits a monotonic ω -linear dependence over a wide energy range up to 0.4 eV in the low- T coherent region.⁴⁸

(3) The Al impurity affects the optical spectrum over the entire energy range up to 1 eV or higher, which is contrary to the simple Drude response. This variation also can be well described by $\gamma^*(\omega)$.

In the one-component scenario, the slowly decaying quasi-Drude response in the low- T coherent region is naturally interpreted to originate from the diffusive character inherent in the doped carriers and to cross over to the finite-energy peak in the high- T incoherent region. In addition, because the pronounced quasi-Drude peak consists of a single collective excitation of the charge carriers, the spectral weight associated with the charge transport, or the *Drude weight*, is estimated to be 0.2–0.3 per Mn atom at the lowest temperature (it depends on the estimate of the contribution from the interband excitations^{7,16}), which is consistent with the Hall effect^{49,50} and specific heat⁵¹ studies. In contrast, in the two-component picture, the Drude weight is estimated to have an unphysically small value of ~ 0.02 per Mn atom,^{11,15} though it is partly due to the deterioration of the sample surfaces.

The most significant characteristic of the charge dynamics in the low- T coherent region is ω linearity in γ^* over a wide energy range. [We have been unable to find a previous (theoretical) study reporting the ω dependence of γ^* .] However, contrary to optimally doped high-temperature superconductors ($\gamma^* \propto \omega$ and $\rho \propto T$)² and heavy-fermion systems ($\gamma^* \propto \omega^2$ and $\rho \propto T^2$),⁴⁷ there is a discrepancy between the ac and dc conductivities for manganites; the temperature dependence of the low- T resistivity has been variously reported to be $\rho \propto T^2$,^{40,52} $\rho \propto T^3$,⁵³ or $\rho \propto 1/\sinh^2(\hbar\omega_s/2k_B T)$,⁵⁴ but T -linear resistivity has not been reported yet.⁵⁵ This discrepancy may originate from the difference in the energy scale. For the manganites, the discussion on the T dependence of the resistivity is limited at low temperatures ($k_B T < 100$ K), which are much smaller energies than the energy scale in the discussion on γ^* ($\hbar\omega \gtrsim 0.1$ eV). At such low temperatures, there is a ferromagnetic ordering and hence additional factors such as magnon scattering may be predominant.⁵⁶ In contrast, for high-temperature superconductors and heavy-fermion systems the energy scale is coincident between the

ac and dc conductivities. Also for another bad metal SrRuO_3 ,^{57,58} $\rho(T)$ exhibits T -superlinear behavior at low temperatures, where the material is ferromagnetically ordered, which is incompatible with its ω linearity in γ^* ,⁵⁹ but above $T_C \sim 160$ K the resistivity exhibits the T -linear behavior. Another reason for the discrepancy may be the change in ω_p or the Drude weight with temperature. The T dependence of $\rho(T)$ for the manganites may be governed not only by the scattering rate at the high temperatures in the vicinity of T_C .

B. Coherent-to-incoherent crossover

One of the important implications of the present experiment is a relationship between the coherent-to-incoherent crossover in $\sigma(\omega)$ and the Mott criterion in σ_{dc} . The Mott criterion σ_{Mott} of $\text{La}_{1-x}\text{Sr}_x\text{MnO}_3$ is suggested to be $2000 - 3000 \Omega^{-1}\text{cm}^{-1}$, which is universal for all x , from the study of the Al-impurity effect on the resistivity.³⁷ The present optical study shows that the crossover temperature T^* is about 300 K for $x=0.4$ and about 200 K for $x=0.175$. For both compounds σ_{dc} is $1600 - 1800 \Omega^{-1}\text{cm}^{-1}$ around T^* . The discrepancy is not significant because the coherent-to-incoherent crossover is not a sharp transition and also because the estimation of σ_{Mott} involves some ambiguity.⁶⁰ As is described above, such a finite-energy peak in $\sigma(\omega)$ is incompatible with the coherent motion of the charge carriers. It is well known that the finite-energy peak is a characteristic of the hopping conduction in a disordered⁶¹ or a polaronic⁶² system. Therefore, the relation to σ_{Mott} substantiates that the present finite-energy peak above T^* is due to some scattering process, or a kind of localization. The condition of *low-T* Anderson localization $l \sim \lambda_F$ (or $\sigma_{dc} \sim \sigma_{\text{Mott}}$) (Ref. 39) seems to be important also in the present *high-T* crossover. For the manganites, $\rho(T)$ exhibits the anomaly at T_C , suggesting that the ferromagnetic transition is related to the change of the transport. However, $\sigma(\omega)$ and $\gamma^*(\omega)$ demonstrate that σ_{Mott} or l dominates more directly the charge transport and/or the scattering process.

Although the simple double-exchange model does not explain the insulating behavior above T_C ,^{37,40,52} it can explain the bad metallic resistivity itself.^{18,63} Therefore, the wide-band $\text{La}_{0.6}\text{Sr}_{0.4}\text{MnO}_3$ has been regarded as a conventional double-exchange system. However, the simple double-exchange model predicts a (simple) Drude response in $\sigma(\omega)$ over the entire temperature range,¹⁸ contrary to the present result. The additional physics such as the dynamical Jahn-Teller polaronic^{8,19} or bipolaronic²³ effect, e_g -orbital degrees of freedom,^{20,21,24} charge ordering instability,⁶⁴ and electronic repulsion²⁹ are important even for the wide-band manganites. A dynamical mean-field theory of the double-exchange model incorporating the dynamical Jahn-Teller effect¹⁹ can qualitatively explain the high- T finite-energy peak as well as the low- T quasi-Drude peak. In this scenario, the crossover is regarded as the crossover from low- T mobile to high- T immobile polarons. In addition, this theory also predicts that the coherent-to-incoherent crossover in $\sigma(\omega)$ occurs below T_C for a certain strength of the coupling con-

stant. The relevance to σ_{Mott} and the ω linearity in γ^* can be significant experimental constraints on future theoretical studies.

C. Comparison to other bad metals

A similar coherent-to-incoherent crossover in $\sigma(\omega)$ is also observed for other prototypical bad metals, SrRuO_3 (Ref. 59) and $\text{La}_{2-x}\text{Sr}_x\text{CuO}_4$,⁶⁵ and is suggested for $\text{Bi}_2\text{Sr}_2\text{CuO}_6$.⁶⁶ Also for these bad metals, the relation between the crossover and σ_{Mott} is suggested.⁶⁷ Although the quasi-Drude response below T^* is observed universally for almost all the correlated or bad metals, the finite-energy peak above T^* has not been generally confirmed yet. However, if $\rho(T)$ increases (σ_{dc} decreases) with increasing temperature without saturation, while $R(\omega)$ still shows an edge at high temperatures, which produces a spectral weight at lower energies, the finite-energy peak inevitably appears in $\sigma(\omega)$ at high temperatures. In contrast, if $\rho(T)$ saturates at high temperatures, which is considered as a general characteristic of ordinary metals,⁶⁸ $\sigma(\omega)$ is expected to exhibit a rather weak temperature dependence and to keep the (simple) Drude behavior at the high temperatures. In this sense, the absence of resistivity saturation is inseparably related to the appearance of the finite-energy peak in $\sigma(\omega)$. Therefore, the characteristics of bad metals may be summarized as follows: (i) absence of resistivity saturation, (ii) a slowly decaying quasi-Drude peak in $\sigma(\omega)$ at low temperatures, and (iii) a finite-energy peak in $\sigma(\omega)$ at high temperatures. The second characteristic can be expressed more quantitatively as $\gamma^* \propto \omega$. This is named the ‘‘marginal’’ Fermi-liquid response,⁶⁹ which is different from either the noninteracting (ω independent) or the electron-electron scattering ($\gamma^* \propto \omega^2$) case.

Because the crossover occurs at high temperatures where inelastic scattering is strong, and also because the residual resistivity is small and the resistivity remains metallic even at the lowest temperature for these materials, the present finite-energy peak is distinct from the low- T Anderson localization caused by elastic scattering due to (extrinsic) disorder. In this sense, the present phenomenon is what is called ‘‘dynamical’’ localization⁵⁹ and is due to some strong (intrinsic) inelastic scattering. The universality in the phenomena suggests the universality in the mechanism, but no general concept for the origin of the present crossover is established to date. For doped Mott insulators, the physics relevant to the insulating nature of the nondoped material, which subsists even in the doped metallic region, probably plays some role. (For the manganites, the above-mentioned additional physics are the candidates of the origin.) For stoichiometric SrRuO_3 , a recent theoretical study predicts that t_{2g} -orbital degrees of freedom can be an origin of the strong intrinsic scattering.⁷⁰

The crossover observed for $\text{La}_{1-x}\text{Sr}_x\text{MnO}_3$ is much clearer than that observed for other bad metals. For SrRuO_3 , the finite-energy peak at high temperatures is not so remarkable, the upturn of γ^* is limited to lower energies (below 250 cm^{-1}), and the peak position is much smaller (below 200 cm^{-1}).⁵⁹ The crossover in $\text{La}_{2-x}\text{Sr}_x\text{CuO}_4$ (Ref. 65) resembles that in SrRuO_3 . The phenomenon in $\text{La}_{1-x}\text{Sr}_x\text{MnO}_3$ is clearly defined as the (dynamical) localization, while that

in SrRuO_3 and $\text{La}_{2-x}\text{Sr}_x\text{CuO}_4$ is more itinerant and may be defined as “quasi-localization.” This may be inherent to the perfect half-metallic state (the strong Hund’s coupling) and/or due to the strong additional physics in the manganites.

V. CONCLUDING REMARKS

We have reviewed the dynamics of the charge carriers doped onto a prototypical double-exchange ferromagnet $\text{La}_{1-x}\text{Sr}_x\text{MnO}_3$ based on the optical spectra obtained at cleaved surfaces of the single crystals. The significant findings of the present study are summarized as follows.

(1) The optical conductivity $\sigma(\omega)$ in the ferromagnetic-metallic state is characterized by the coherent-to-incoherent crossover. $\sigma(\omega)$ exhibits a zero-energy, slowly decaying quasi-Drude peak at low temperatures, but above a certain temperature T^* the quasi-Drude peak shifts to the finite-energy region regardless of the metallic resistivity. A relationship between the crossover in $\sigma(\omega)$ and the Mott criterion in σ_{dc} is also suggested.

(2) The Al-substitution effect on the optical spectrum is not limited within the low-energy region but extends up to 1 eV or higher. This is contrary to the prediction from the simple Drude picture.

(3) The frequency-dependent scattering rate $\gamma^*(\omega)$ deduced by an extended Drude analysis well describes the

overall feature of the charge dynamics. In particular, the charge dynamics at a low- T coherent region is characterized by an anomalous ω -linear scattering rate $\gamma^*(\omega)$ over a wide energy range up to 0.4 eV.

These features seem to support that the one-component model offers a more useful description of the charge dynamics. From this viewpoint, the slowly decaying quasi-Drude term in $\sigma(\omega)$, which is commonly observed for almost all the correlated or bad metals, can be reasonably assigned as a single collective excitation of the charge carriers with a highly diffusive character. The finite-energy peak at high temperatures, on the other hand, is an indication of the dynamical localization state. The charge dynamics continuously changes from the low- T coherent to high- T incoherent regimes.

ACKNOWLEDGMENTS

We are grateful to S. Uchida, H. Takagi, and Ross H. McKenzie for their helpful comments. We also would like to thank Y. Sawaki, A. Osuka, and S. Okuyama for their help in the experiments. This work was financially supported by a Grant-in-Aid for Scientific Research from the Ministry of Education, Culture, Sports, Science and Technology of Japan, by CREST of JST, and by the DAIKO Foundation.

*Author to whom correspondence should be addressed. Electronic address: k46291a@nucc.cc.nagoya-u.ac.jp

¹F. Wooten, *Optical Properties of Solids* (Academic Press, New York, 1972).

²Z. Schlesinger, R. T. Collins, F. Holtzberg, C. Feild, G. Koren, and A. Gupta, *Phys. Rev. B* **41**, 11 237 (1990).

³J. Orenstein, G. A. Thomas, A. J. Millis, S. L. Cooper, D. H. Rapkine, T. Timusk, L. F. Schneemeyer, and J. V. Waszczak, *Phys. Rev. B* **42**, 6342 (1990).

⁴For reviews, see S. Uchida, H. Eisaki, and S. Tajima, *Physica B* **186-188**, 975 (1993); T. Timusk, *Physica C* **317-318**, 18 (1999).

⁵D. B. Tanner and T. Timusk, in *Physical Properties of High Temperature Superconductors III*, edited by D. M. Ginsberg (World Scientific, Singapore, 1992), p. 363.

⁶For a review, see T. A. Kaplan and S. D. Mahanti, *Physics of Manganites* (Plenum, New York, 1999).

⁷Y. Moritomo, A. Machida, K. Matsuda, M. Ichida, and A. Nakamura, *Phys. Rev. B* **56**, 5088 (1997).

⁸M. Quijada, J. Černe, J. R. Simpson, H. D. Drew, K. H. Ahn, A. J. Millis, R. Shreekala, R. Ramesh, M. Rajeswari, and T. Venkatesan, *Phys. Rev. B* **58**, 16 093 (1998).

⁹A. V. Boris, N. N. Kovaleva, A. V. Bazhenov, P. J. M. van Bentum, Th. Rasing, S.-W. Cheong, A. V. Samoilov, and N.-C. Yeh, *Phys. Rev. B* **59**, R697 (1999).

¹⁰H. J. Lee, J. H. Jung, Y. S. Lee, J. S. Ahn, T. W. Noh, K. H. Kim, and S.-W. Cheong, *Phys. Rev. B* **60**, 5251 (1999).

¹¹E. Saitoh, Y. Okimoto, Y. Tomioka, T. Katsufuji, and Y. Tokura, *Phys. Rev. B* **60**, 10 362 (1999).

¹²K. Takenaka, Y. Sawaki, and S. Sugai, *Phys. Rev. B* **60**, 13 011 (1999).

¹³J. R. Simpson, H. D. Drew, V. N. Smolyaninova, R. L. Greene,

M. C. Robson, A. Biswas, and M. Rajeswari, *Phys. Rev. B* **60**, R16 263 (1999).

¹⁴N. Kida, M. Hangyo, and M. Tonouchi, *Phys. Rev. B* **62**, R11 965 (2000).

¹⁵E. Saitoh, A. Asamitsu, Y. Okimoto, and Y. Tokura, *J. Phys. Soc. Jpn.* **69**, 3614 (2000).

¹⁶K. Takenaka, Y. Sawaki, R. Shiozaki, and S. Sugai, *Phys. Rev. B* **62**, 13 864 (2000).

¹⁷A. Congeduti, P. Postorino, P. Dore, A. Nucara, S. Lupi, S. Mercone, P. Calvani, A. Kumar, and D. D. Sarma, *Phys. Rev. B* **63**, 184410 (2001).

¹⁸N. Furukawa, *J. Phys. Soc. Jpn.* **64**, 3164 (1995); see also T. A. Kaplan and S. D. Mahanti, *Physics of Manganites* (Ref. 6), p. 1.

¹⁹A. J. Millis, R. Mueller, and Boris I. Shraiman, *Phys. Rev. B* **54**, 5405 (1996).

²⁰S. Ishihara, M. Yamanaka, and N. Nagaosa, *Phys. Rev. B* **56**, 686 (1997).

²¹P. E. de Brito and H. Shiba, *Phys. Rev. B* **57**, 1539 (1998).

²²S. Yunoki, A. Moreo, and E. Dagotto, *Phys. Rev. Lett.* **81**, 5612 (1998).

²³A. S. Alexandrov and A. M. Bratkovsky, *Phys. Rev. Lett.* **82**, 141 (1999).

²⁴P. Horsch, J. Jaklič, and F. Mack, *Phys. Rev. B* **59**, 6217 (1999).

²⁵V. Ferrari, M. J. Rozenberg, and R. Weht, cond-mat/9906131 (unpublished).

²⁶M. O. Dzero, L. P. Gor’kov, and V. Z. Kresin, *Eur. Phys. J. B* **14**, 459 (2000).

²⁷A. Chattopadhyay, A. J. Millis, and S. Das Sarma, *Phys. Rev. B* **61**, 10 738 (2000).

²⁸H. Nakano, Y. Motome, and M. Imada, *J. Phys. Soc. Jpn.* **69**, 1282 (2000).

- ²⁹K. Held and D. Vollhardt, Phys. Rev. Lett. **84**, 5168 (2000).
- ³⁰Y. Imai and N. Kawakami, J. Phys. Soc. Jpn. **69**, 3063 (2000).
- ³¹T. A. Kaplan, S. D. Mahanti, and Y.-S. Su, Phys. Rev. Lett. **86**, 3634 (2001).
- ³²L. D. Rotter, Z. Schlesinger, R. T. Collins, F. Holtzberg, C. Field, U. Welp, G. W. Crabtree, J. Z. Liu, Y. Fang, K. G. Vandervoort, and S. Fleshler, Phys. Rev. Lett. **67**, 2741 (1991).
- ³³Z. Schlesinger, R. T. Collins, L. D. Rotter, F. Holtzberg, C. Field, U. Welp, G. W. Crabtree, J. Z. Liu, Y. Fang, K. G. Vandervoort, and S. Fleshler, Physica C **235-240**, 49 (1994).
- ³⁴D. N. Basov, R. Liang, B. Dabrowski, D. A. Bonn, W. N. Hardy, and T. Timusk, Phys. Rev. Lett. **77**, 4090 (1996).
- ³⁵For a review, see T. Timusk and B. Statt, Rep. Prog. Phys. **62**, 61 (1999).
- ³⁶V. J. Emery and S. A. Kivelson, Phys. Rev. Lett. **74**, 3253 (1995).
- ³⁷Y. Sawaki, K. Takenaka, A. Osuka, R. Shiozaki, and S. Sugai, Phys. Rev. B **61**, 11 588 (2000).
- ³⁸The present definition of “bad metals” follows that by Emery and Kivelson (Ref. 36), that is, a bad metal fails to exhibit the resistivity saturation even when $\rho(T)$ becomes comparable with (and/or much larger than) $\rho_{\text{Mott}} = \sigma_{\text{Mott}}^{-1}$, at which l is comparable with λ_F . This suggests the breakdown of the conventional Bloch-Boltzmann transport mechanism, and hence its origin and transport mechanism there are now attracting great attention. See, for example, A. J. Millis, J. Hu, and S. Das Sarma, Phys. Rev. Lett. **82**, 2354 (1999); J. Merino and R. H. McKenzie, Phys. Rev. B **61**, 7996 (2000). In this definition, $\text{La}_{0.6}\text{Sr}_{0.4}\text{MnO}_3$ is classified as a bad metal.
- ³⁹N. F. Mott, *Metal-Insulator Transitions*, 2nd ed. (Taylor & Francis, London, 1990).
- ⁴⁰A. Urushibara, Y. Moritomo, T. Arima, A. Asamitsu, G. Kido, and Y. Tokura, Phys. Rev. B **51**, 14 103 (1995).
- ⁴¹R. Shiozaki, K. Takenaka, Y. Sawaki, and S. Sugai, Phys. Rev. B **63**, 184419 (2001).
- ⁴²K. Takenaka, Y. Sawaki, and S. Sugai, J. Phys. Soc. Jpn. **70**, 1896 (2001).
- ⁴³O. R. Mercier, R. G. Buckley, A. Bittar, H. J. Trodahl, E. M. Haines, J. B. Metson, and Y. Tomioka, Phys. Rev. B **64**, 035106 (2001).
- ⁴⁴K. Takenaka, K. Iida, Y. Sawaki, S. Sugai, Y. Moritomo, and A. Nakamura, J. Phys. Soc. Jpn. **68**, 1828 (1999).
- ⁴⁵In this framework, the highest exchange-gap excitation assigned to $t_{2g}\uparrow \rightarrow e_g\downarrow$ is predicted to exist at about 7 eV. However, $N_{\text{eff}}^*(\omega)$ suggests that the spectral weight associated with this excitation is small (inset of Fig. 3).
- ⁴⁶P. B. Allen, W. E. Pickett, and H. Krakauer, Phys. Rev. B **37**, 7482 (1988).
- ⁴⁷B. C. Webb, A. J. Sievers, and T. Mihalisin, Phys. Rev. Lett. **57**, 1951 (1986).
- ⁴⁸A similar argument has been made for high-temperature superconductors; T. Timusk, A. V. Puchkov, D. N. Basov, and T. Startseva, J. Phys. Chem. Solids **59**, 1953 (1998).
- ⁴⁹P. Matl, N. P. Ong, Y. F. Yan, Y. Q. Li, D. Studebaker, T. Baum, and G. Doubinina, Phys. Rev. B **57**, 10 248 (1998).
- ⁵⁰A. Asamitsu and Y. Tokura, Phys. Rev. B **58**, 47 (1998).
- ⁵¹J. M. D. Coey, M. Viret, L. Ranno, and K. Ounadjela, Phys. Rev. Lett. **75**, 3910 (1995).
- ⁵²T. Okuda, A. Asamitsu, Y. Tomioka, T. Kimura, Y. Taguchi, and Y. Tokura, Phys. Rev. Lett. **81**, 3203 (1998).
- ⁵³T. Akimoto, Y. Moritomo, A. Nakamura, and N. Furukawa, Phys. Rev. Lett. **85**, 3914 (2000).
- ⁵⁴G.-M. Zhao, V. Smolyaninova, W. Prellier, and H. Keller, Phys. Rev. Lett. **84**, 6086 (2000).
- ⁵⁵The temperature dependence of the low- T resistivity depends on the sample quality. Recent studies using well-characterized samples report the deviation from the T^2 dependence (Refs. 37, 53, and 54). However, these resistivity data can be well fitted by either $\rho \propto T^3$ or $\rho \propto 1/\sinh^2(\hbar\omega_s/2k_B T)$, and hence it is difficult to determine the mechanism only from the fitting analysis.
- ⁵⁶N. Furukawa, J. Phys. Soc. Jpn. **69**, 1954 (2000).
- ⁵⁷L. Klein, J. S. Dodge, C. H. Ahn, G. J. Snyder, T. H. Geballe, M. R. Beasley, and A. Kapitulnik, Phys. Rev. Lett. **77**, 2774 (1996).
- ⁵⁸P. B. Allen, H. Berger, O. Chauvet, L. Forro, T. Jarlborg, A. Junod, B. Revaz, and G. Santi, Phys. Rev. B **53**, 4393 (1996).
- ⁵⁹P. Kostic, Y. Okada, N. C. Collins, Z. Schlesinger, J. W. Reiner, L. Klein, A. Kapitulnik, T. H. Geballe, and M. R. Beasley, Phys. Rev. Lett. **81**, 2498 (1998).
- ⁶⁰The discrepancy may be explained by the possible overestimation of σ_{Mott} . In Ref. 37, σ_{Mott} is defined as the critical σ_{dc} value for the upturn in $\rho(T)$ at low temperatures, which is an indication of the localization caused by the Al doping. The effect of the weak localization may cause an upturn at l slightly larger than λ_F (Ref. 39).
- ⁶¹A. Gold, S. J. Allen, B. A. Wilson, and D. C. Tsui, Phys. Rev. B **25**, 3519 (1982).
- ⁶²H. G. Reik and D. Heese, J. Phys. Chem. Solids **28**, 581 (1967).
- ⁶³S. Ishizaka and S. Ishihara, Phys. Rev. B **59**, 8375 (1999).
- ⁶⁴P. Schiffer, A. P. Ramirez, W. Bao, and S.-W. Cheong, Phys. Rev. Lett. **75**, 3336 (1995).
- ⁶⁵K. Takenaka, R. Shiozaki, S. Okuyama, J. Nohara, A. Osuka, Y. Takayanagi, and S. Sugai, Phys. Rev. B **65**, 092405 (2002).
- ⁶⁶A. A. Tsvetkov, J. Schützmann, J. I. Gorina, G. A. Kaljushnaia, and D. van der Marel, Phys. Rev. B **55**, 14 152 (1997).
- ⁶⁷There is an argument opposing the relation between the crossover and σ_{Mott} for $\text{La}_{2-x}\text{Sr}_x\text{CuO}_4$. T. Startseva *et al.* reported that even highly doped, low-resistivity $\text{La}_{1.78}\text{Sr}_{0.22}\text{CuO}_4$ exhibits a similar finite-energy peak in $\sigma(\omega)$ at room temperature [T. Startseva, T. Timusk, M. Okuya, T. Kimura, and K. Kishio, Physica C **321**, 135 (1999)]. However, no other previous studies reported the appearance of the finite-energy peak at that temperature for the highly doped region [for example, S. Uchida, T. Ido, H. Takagi, T. Arima, Y. Tokura, and S. Tajima, Phys. Rev. B **43**, 7942 (1991)]. See also Ref. 65.
- ⁶⁸Z. Fisk and G. W. Webb, Phys. Rev. Lett. **36**, 1084 (1976); H. M. Milchberg, R. R. Freeman, S. C. Davey, and R. M. More, *ibid.* **61**, 2364 (1988).
- ⁶⁹C. M. Varma, P. B. Littlewood, S. Schmitt-Rink, E. Abrahams, and A. E. Ruckenstein, Phys. Rev. Lett. **63**, 1996 (1989).
- ⁷⁰M. S. Laad and E. Müller-Hartmann, Phys. Rev. Lett. **87**, 246402 (2001).